

T_1 relaxation times in glycerin samples of varying concentration

Tim Foldy-Porto¹ and Stuart Nicholls¹

Dept. of Physics, Yale University

(Dated: 19 December 2019)

In this study, we show that there is a linear relationship between the concentration of glycerine in a sample and T_1 , the sample’s thermal relaxation time under pulsed nuclear magnetic resonance (pNMR) imaging. Using a .4T magnetic field, we performed measurements of T_1 on mixtures of glycerin and water. As expected, we found that T_1 scaled linearly with the ratio of glycerine to water. The relationship between the two variables—concentration of glycerine G and T_1 —is described by: $T_1 = 346.68 - 3.27G$. Due to the linearity of T_1 with respect to the volume of glycerine, we conclude that the two substances, glycerine and water, are negligibly reactive with each other and that the NMR technique is a promising method for testing the purity of a glycerin solution.

I. INTRODUCTION

NMR is a widely used experimental technique to recover nuclear information about an unknown or physically obscured sample. For instance, NMR is used by chemists to determine the identity of an unknown compound and by doctors to image the inside of the human body. The physical principle behind NMR—the absorption of RF energy by a nucleus when in the presence of a magnetic field—was first observed by Isidor Rabi in 1938¹. The technique was further developed in 1946 by Edward Purcell² and Felix Bloch³. Independently, Bloch and Purcell refined the method used by Rabi so that they could sample solids and liquids, as opposed to a molecular beam that Rabi used as his sample. All three physicists won the Nobel prize for their efforts, with Rabi winning in 1944 and Purcell and Bloch winning jointly in 1952.

Use of pulsed NMR to measure viscosity of a liquid (for which the concentration of glycerin is a close proxy), is not a new idea. As early as 1961, Brown measured proton relaxation times in crude oils and found a close correlation between the viscosity of a crude oil and its relaxation time⁴. In 1965, Ragozzino measured the effect of glycerin concentration in water on relaxation time and found an apparently strong correlation, although only four data points were taken⁵. More recently, Lo et. al. measured the relationship of viscosity, diffusivity and gas/oil ratio to the relaxation times of methane and hydrocarbon mixtures. This has applications in petroleum engineering, as the “Viscosity, diffusivity, relaxation time and gas/oil ratio are important properties in the characterization of reservoirs by NMR well logging and in prediction of production performance.”⁶

In essence, the NMR technique allows researchers to obtain information about the spin component of the sample material as well as information about the locations of the nuclei inside it. While the spins of the component nuclei take on discrete values, namely $\pm\frac{1}{2}$, the aggregate spin can take on an essentially continuous range of values. This net spin can be represented by a vector in a three-dimensional space, the Bloch sphere, where the magnitude indicates the level of coherence of the component spins. By placing the sample in an external mag-

netic field, one can force this net-spin vector to precess around the axis along which the field points (say \hat{z}), an effect known as Larmor precession. Then, in applying a carefully tuned RF pulse perpendicular to the external field, the net-spin vector is tipped into the XY plane. The frequency at which these spins are affected by this technique, called the *resonant frequency*, is unique to the composition of the sample; resonance occurs at different frequencies for different nuclei.

After the spins have been tipped, one can measure the projection of the net-spin vector into the XY plane using a complicated apparatus which will be explained in section two. At that point the work is almost done: the only thing remaining is to observe the behavior of that projection, from which one can determine various properties of the sample.

A. A more rigorous description of NMR

For simplicity, consider the behavior of a single particle in an external field of strength B_0 . The field couples with the spin of the particle according to the Hamiltonian

$$\hat{H} = -\gamma\mathbf{B} \cdot \mathbf{S} = -\gamma B_z S_z \hat{z} \quad (1)$$

Where γ is the gyromagnetic ratio, and in the last step we assume that the external field points in the \hat{z} direction. According to Ehrenfest’s theorem

$$\frac{d\langle\mathbf{S}\rangle}{dt} = \gamma\langle\mathbf{S} \times \mathbf{B}\rangle \quad (2)$$

After a bit of manipulation, we get

$$\frac{d^2\langle S_x \rangle}{dt^2} = -(\gamma B_z)^2 \langle S_x \rangle \quad (3)$$

We get a similar equation for S_y , and taken together, the two equations describe precession of the spin around \hat{z} with frequency γB_0 (the resonant frequency).

Statistical mechanics tells us that if a sample is left in this external field for long enough, almost all of its spins

will have aligned with \hat{z} . In order to achieve the tipping of the spins into the XY plane, one must apply an oscillating pulse in the perpendicular direction, as mentioned previously. The math behind this is a bit messy, but illuminating.

The behavior of a single particle with wavefunction $\Psi(x, t)$ is determined by the Schrodinger equation

$$i\hbar \frac{d\Psi}{dt} = \hat{H}\Psi \quad (4)$$

When we apply a perpendicular pulse, say, in \hat{x} , our Hamiltonian becomes

$$\hat{H} = -\frac{\hbar^2}{2m}\nabla^2 - \gamma B_z S_z + \gamma B_x \cos(\omega t) S_x \quad (5)$$

The first term is the usual operator for kinetic energy and the middle term is the coupling with static magnetic field in \hat{z} from equation 1. The final term represents a time oscillating pulse with frequency ω in \hat{x} . Next, we explicitly write S_x and S_z as matrix operators in the basis of S_z eigenstates

$$S_x = -\frac{\hbar}{2} \begin{bmatrix} 0 & 1 \\ 1 & 0 \end{bmatrix} \quad S_z = -\frac{\hbar}{2} \begin{bmatrix} 1 & 0 \\ 0 & -1 \end{bmatrix} \quad (6)$$

Finally, before we put everything together, let's assume that Ψ takes the form

$$\Psi(t) = \begin{bmatrix} c_1(t) \\ c_2(t) \end{bmatrix} \quad (7)$$

The Schrodinger equation now reads

$$i\hbar \begin{bmatrix} \dot{c}_1 \\ \dot{c}_2 \end{bmatrix} = -\frac{\hbar}{2} \begin{bmatrix} \frac{\hbar}{m}\nabla^2 + \gamma B_z & \gamma B_x \cos(\omega t) \\ \gamma B_x \cos(\omega t) & \frac{\hbar}{m}\nabla^2 + \gamma B_z \end{bmatrix} \begin{bmatrix} c_1 \\ c_2 \end{bmatrix} \quad (8)$$

Now, to make the equation easier to solve and to make the solution more physically meaningful, let's transform Ψ into the rotating frame. The transformation is

$$\begin{bmatrix} c_1 \\ c_2 \end{bmatrix} \rightarrow \begin{bmatrix} c_1^r e^{i\omega t/2} \\ c_2^r e^{-i\omega t/2} \end{bmatrix} \quad (9)$$

Where c_1^r and c_2^r are the coefficients of the x and y components, respectively, of Ψ in the frame of precession around \hat{z} . In this new coordinate system, equation 8 looks like

$$i\hbar \begin{bmatrix} (\dot{c}_1^r + \frac{i\omega t}{2})e^{i\omega t/2} \\ (\dot{c}_2^r - \frac{i\omega t}{2})e^{-i\omega t/2} \end{bmatrix} = -\frac{\hbar}{2} \begin{bmatrix} \frac{\hbar}{m}\nabla^2 + \gamma B_z & \gamma B_x \cos(\omega t) \\ \gamma B_x \cos(\omega t) & \frac{\hbar}{m}\nabla^2 + \gamma B_z \end{bmatrix} \begin{bmatrix} c_1^r e^{i\omega t/2} \\ c_2^r e^{-i\omega t/2} \end{bmatrix} \quad (10)$$

We can solve this matrix equation to get two coupled differential equations in c_1^r and c_2^r . After solving them and substituting Ψ back in, we get

$$i\hbar |\Psi\rangle = [-\frac{\hbar}{2}(\gamma B_z - \omega)S_z - \gamma B_x S_x] |\Psi\rangle \quad (11)$$

Remember that this is the solution for a person observing in the rotating frame; the direction of the net-spin vector remains constant for them, even though it precesses around \hat{z} for a person observing from the laboratory frame. From equation 11, we can see that if ω , the frequency of the oscillating magnetic field applied in \hat{x} , is the same as the resonant frequency with which the net-spin vector precesses around \hat{z} , the S_z term goes away and Ψ is acted on only by $-\gamma B_x S_x$. To the observer in the rotating frame, it appears that the sample is acted upon by a static field in \hat{x} , so the net-spin vector exhibits Larmor precession around \hat{x} . This is the tipping of the spins for which we sought a mathematical explanation. It turns out that all you have to do to rotate the spins into the XY plane, where they can be measured, is apply a magnetic field (perpendicular to the static field) that oscillates at the sample's resonant frequency. If the oscillating field is applied for just the right duration of time, one can control the angle that the spins tip into the XY plane. In our experiment, we tipped the spins 90° (a " $\frac{\pi}{2}$ pulse") and 180° (a " π pulse"). Both of these pulse types are shown in figure 1.

B. Relaxation times, free induction decay, and spin echoes

There are three additional features of NMR which are of relevance to our experiment: relaxation times, free induction decay, and spin echoes. When the spins are tipped into the XY plane, as described in the previous section, they don't stay there indefinitely. Through a variety of processes, the individual spins begin to decohere, resulting in a reduction of magnitude of the net-spin vector. These processes are labeled according to their characteristic relaxation times, T_1 , T_2 , and T_2^* . T_2^* is the fastest decay process, characterizing the decoherence of the spins due to the non-uniformity of B_z . T_2 decay is slower than T_2^* but faster than T_1 . It is caused by dipole-dipole coupling of the various spins. T_1 is the slowest decay mechanism; it refers to the sample returning to thermal equilibrium, in which all the spins point along \hat{z} . T_2^* and T_2 are visualized in panel (c), (d), and (e) of figure 1.

Free induction decay (hereafter referred to as FID) is the process by which a net-spin vector returns to \hat{z} after being tipped into the XY plane. Though T_1 , T_2 , and T_2^* all contribute to this decay, T_2^* is dominant and thus FID can often be characterized as a decaying exponential e^{-t/T_2^*} . To reiterate, this function represents the magnitude of the projection of the net-spin vector into the

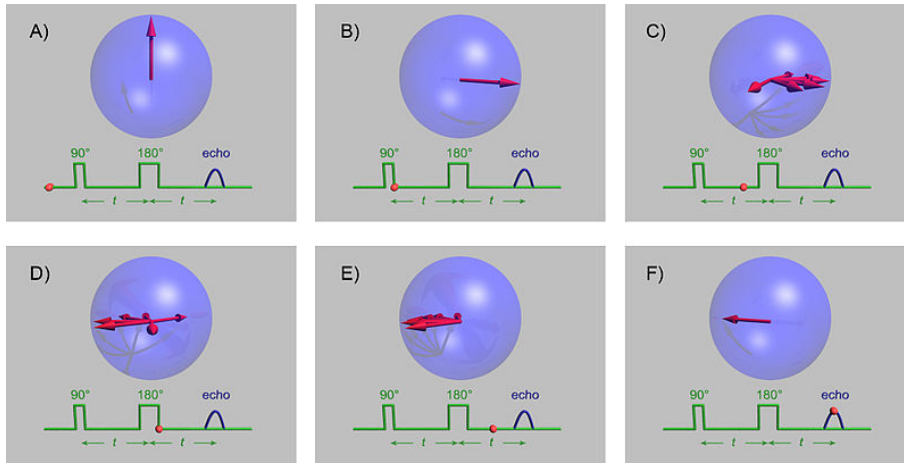


FIG. 1. In this diagram, we are in the frame of reference that rotates at the resonant frequency of the sample. **a**: The spins initially point in \hat{z} **b**: A $\frac{\pi}{2}$ pulse tips the spins into the XY plane **c**: The spins decohere in the XY plane due to local variations in the static magnetic field **d**: A π pulse inverts the spins in the XY plane **e**: The spins begin to re-cohere due to the same local variations as in (c) **f**: The spins re-cohere completely and the net-spin vector experiences a resurgence in magnitude, which is observed as a spin echo.

XY plane. If our oscillating pulse in \hat{x} is detuned from the resonant frequency, we will observe decaying oscillations, the frequency of which will be that of the beat frequencies.

Although it can be quite frustrating for one to see their nice coherent spins disappear so quickly, fear not, for the method of spin echoes provides a way to re-cohere spins for further measurement. T_2^* decay ensures that spins in different locations in an inhomogeneous field will precess at different rates. After the spins are initially tipped into the XY plane, they decohere according to T_2^* . If a π pulse is then applied (rotating the spins 180° around \hat{x}), then the spins, having been inverted in the XY plane, will actually begin to “decohere” back together again. This effect is made possible by the position-dependency of T_2^* —should the spins be translated in space, rather than rotated, they would not re-cohere at the same rate that they each initially decohered, and they would remain in an unobservable decoherent state. Spin echoes are shown in panels (c) through (f) in figure 1.

Although we only measured T_1 in this experiment, the method of spin echoes allowed us to tune our apparatus such that T_2 and T_2^* effects did not interfere with our measurement process.

II. METHODS

A. Preparation of the samples

Ten samples of glycerine were prepared for each trial, with the concentration by volume of the samples ranging from 100% to 45% in even increments of 5%. We created the variable purity samples by mixing glycerine with water in a graduated cylinder. For each sample, we

poured in the glycerine first, measured its volume, then filled the graduated cylinder up with water until it was 10 mL full. We then stirred the solution vigorously until it was properly mixed. Finally, we put five drops of the sample into a small capsule which was inserted into our NMR apparatus for measurement of T_1 .

B. Measuring the sample’s response to NMR

In order to measure T_1 for our samples, we used the existing NMR apparatus built for Yale University in 2010. A block diagram of the apparatus is shown in figure 2. The diagram does not include, however, the large electromagnet that generates the static magnetic field, referenced in section 1.A. as B_z . In order to generate a precisely timed pulse of an oscillating magnetic field, two components are required: a precision pulse generator and an oscillating magnetic field. For the latter, we used a function generator outputting a 6.436356 MHz sine wave with an amplitude of 3.25V peak-to-peak. Through calculation and trial and error, we found this frequency to be the resonant frequency of the sample, and this amplitude to generate the necessary B_x to tip the spins. We then used computer controlled switches to shape this wave into the precisely timed pulses needed to tip the spins 90° and 180° .

In order to deliver these pulses to the sample, we used a small circuit containing some diodes, an inductor, a $\lambda/4$ cable, and an LC filter. The sample is placed inside the inductor, and as a pulse is passed through the inductor, an oscillating magnetic field is produced across the sample. The spins in the sample precess accordingly, and in doing so generate a small back EMF in the inductor, proportional to the spins’ projection into the XY plane. This response signal is filtered out from the pulse via the

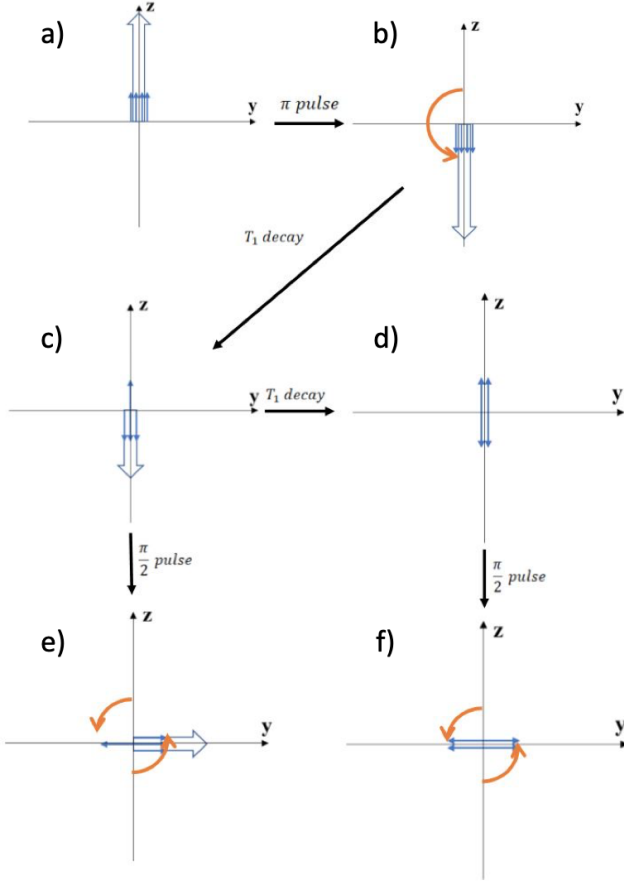


FIG. 2. Determining T_1 from the the sample’s response. **a**: Initially, the spins are coherent along $+\hat{z}$ **b**: A π pulse tips them uniformly into $-\hat{z}$ **c**: The individual spins begin to flip back into $+\hat{z}$; the net-spin vector gradually decreases in magnitude, still pointing along $-\hat{z}$ **d**: At $\tau = \frac{T_1}{\ln(2)}$, half the spins have flipped, meaning the net-spin vector is zero **e**: If a $\frac{\pi}{2}$ pulse is applied after (c), the net-spin vector will exhibit FID **f**: If a $\frac{\pi}{2}$ pulse is applied after (d), the net-spin vector is zero and thus no FID will be observed.

$\lambda/4$ cable and the LC filter. Once the response signal of the sample has been isolated, it is amplified and sent to the oscilloscope for measurement.

C. Determining T_1 from the sample’s response

We found T_1 for each sample using the method “inversion recovery.” The pulse sequence for this method is

$$\pi \rightarrow \tau \rightarrow \frac{\pi}{2} \quad (12)$$

Where τ is a variable amount of time that, when chosen correctly, is related to T_1 by the relationship

$$\tau = \frac{T_1}{\ln(2)} \quad (13)$$

Both equation 13 and the method of choosing the “correct τ ” can be explained using the Bloch sphere. Let’s assume the spins initially point along \hat{z} . After the π pulse, the net-spin vector points along $-\hat{z}$, having been rotated 180° around \hat{x} . As the spins start to decohere uniformly due to T_2 and T_2^* , they also undergo thermal relaxation due to the T_1 process. This results in the net-spin vector receding along $-\hat{z}$, passing through zero, and then growing along $+\hat{z}$ until it returns to its initial value. This process is characterized by exponential decay e^{-t/T_1} . By applying a $\frac{\pi}{2}$ pulse after some time $0 < \tau < T_1$, the net spin vector is tipped into the XY plane where it undergoes FID. If, however, $\tau = T_1/\ln(2)$, the net-spin vector will have recessed exactly halfway between $+\hat{z}$ and $-\hat{z}$, meaning its magnitude will be zero. Therefore, a $\frac{\pi}{2}$ pulse applied after this time will have no effect and no FID will be measured. By sweeping through a range of τ and picking out the one that results in no FID, T_1 can be determined through equation 13. The mechanics of this process are shown in figure 2, while our use of this technique to measure τ is shown in figure 3.

III. RESULTS

Figure 4 represents the variation of T_1 with respect to the concentration of the glycerine samples. We did two trials, fitting to each the linear curve

$$T_1 = T_0 - \alpha G \quad (14)$$

where T_0 is the value of T_1 for a completely pure sample, G is the concentration by volume of glycerine in the samples, and α is a constant of proportionality. The units on T_1 , T_0 , and αG are milliseconds. The results of our two trials are shown in the table below:

	T_0 (ms)	δT_0 (ms)	α (ms)	$\delta \alpha$ (ms)	χ^2
Trial 1	348	± 5	3.29	± 0.06	0.464
Trial 2	345	± 5	3.26	± 0.08	0.749

Since the reduced chi-squared of trial two is much better than that of trial one, we chose to present trial two as our final data.

A. Discussion of error

We estimated our error in the concentration-by-volume of the glycerine sample to be $\pm 2\%$. This came from the fact that the graduated cylinder we were using to create the samples had markings for every 0.2 mL. Since we created 10 mL of each solution, an accuracy of 0.2 mL translated to an accuracy of 2%. There were two sources for the error in our measurement of T_1 : error due to our estimation of which value of τ minimized the FID

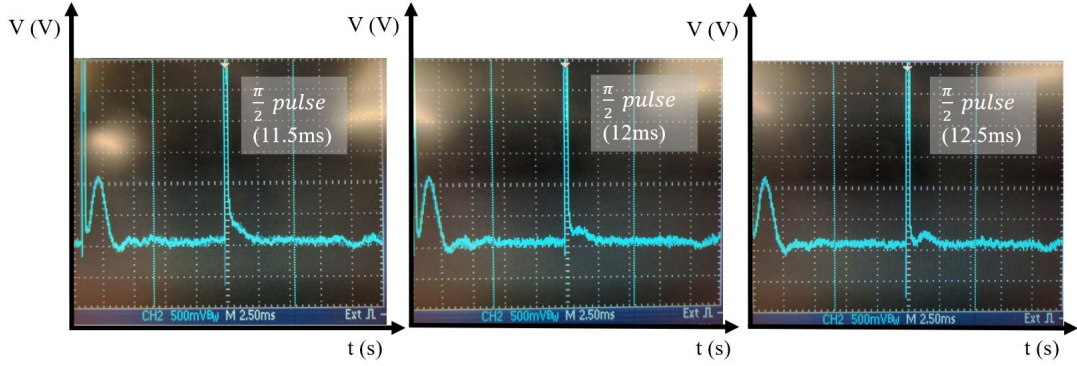


FIG. 3. Oscilloscope screenshots of the inversion recovery method of determining T_1 . Voltage is on the vertical axis (500 mV per division) and time is on the horizontal axis (2.5 ms per division). In each screenshot, the π pulse can be seen as the large vertical line on the left of the screen, and the $\frac{\pi}{2}$ pulse can be seen as the vertical line in the middle of the screen. In the left and right screenshots, τ was slightly above and below the correct value of $\tau = T_1/\ln(2)$, so we observed a bit of FID after the $\frac{\pi}{2}$ pulse. In the middle screenshot, the given τ ended up minimizing the FID response of the sample, meaning that that τ was our best measurement for $T_1/\ln(2)$ for the given sample.

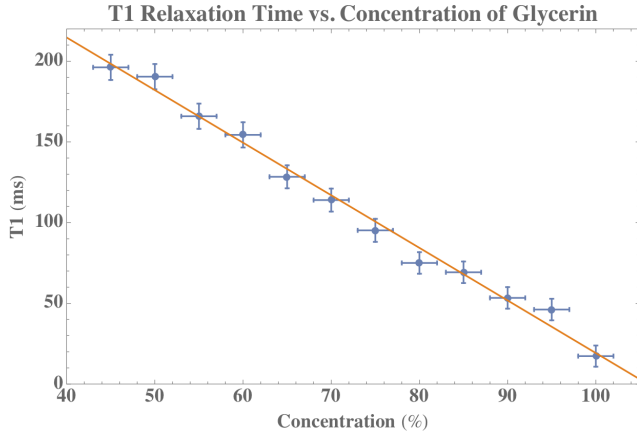


FIG. 4. Variation of T_1 with respect to the concentration of the glycerin samples. The error bars on the horizontal axis come from the degree of accuracy on the graduated cylinder that we used to prepare our samples. To get our error on the vertical axis, we added in quadrature the error in measurement from the inversion recovery technique and the error propagated through from our error in sample concentration.

response, and error propagated from our uncertainty in the concentration of the glycerin samples. We estimated a 2 ms uncertainty (on average) in the FID-minimizing value of τ . This estimate is based on the level of noise present in our measurement. When we were very close (± 2 ms) to the correct value of τ , it was difficult to tell which FID response was minimal. By far, the propagated error from the glycerin concentration was the dominant error, which we determined to be 7 ms (on average). The formula we used for this propagation was

$$\delta y = \sqrt{(\Delta y)^2 + \left(\frac{\partial f}{\partial x} \Delta x\right)^2} \quad (15)$$

$$\delta y = \sqrt{(\Delta y)^2 + (-3.26 \times 2)^2} \quad (16)$$

Where Δy is our uncertainty in the measurement of τ (ranging between 0.5 ms to 3 ms depending on the sample), f is our linear fit ($T_1 = 344.98 - 3.26G$), x is the concentration of glycerine G , and Δx is our uncertainty in G . On average, we found δy to be 7.5 ms.

The fact that our reduced chi-squared is lower than 1 indicates that our data is over-fit. Since we are using a linear fit, and therefore can't reduce the number of fitting parameters any further, we deduced that our estimation of the error was too large. However, we have no quantitative justification for lowering our estimation of the error.

IV. CONCLUSION

The data presented here demonstrate that T_1 is linearly proportional to the concentration of glycerine G according to the relationship

$$T_1 = 345 - 3.26G \quad (\pm 5ms) \quad (17)$$

Since the volume of the samples were held constant, this type of relationship is characteristic of a mixture where the component solutions are unreactive with each other. If the glycerine had reacted with the water it was mixed with, it would have created a new compound which would have altered the T_1 value for the sample (since the nuclei would have been configured differently in the created substance). The creation of this new substance

would have led to a nonlinear relationship between G and T_1 , so our observation of the relationship as linear indicates that no new substance was created.

The fact that we were able to find a good (reduced chi-squared close to 1) linear fit for our data indicates that NMR is a good method for determining the concentration of glycerine in a sample containing unknown amounts of glycerine and water. Our results in this experiment are accurate to the extent that the sample of glycerin used was pure, which could be an undetected source of systematic error. While it is qualitatively very clear that the concentration of glycerin and viscosity of the liquid are tightly related, we have not investigated the exact nature of the relationship (it may linear, for example). This would be a necessary step in order to determine more precisely the effectiveness of measuring T_1 relaxation times to determine the viscosity of a liquid sample.

V. REFERENCES

¹I. I. Rabi, J. R. Zacharias, S. Millman, and P. Kusch, "A New Method of Measuring Nuclear Magnetic Moment," *Physical Re-*

view **53**, 318–318 (1938).

²E. M. Purcell, H. C. Torrey, and R. V. Pound, "Resonance absorption by nuclear magnetic moments in a solid," *Physical review* **69**, 37 (1946).

³F. Bloch, W. Hansen, and M. Packard, "Nuclear induction," *Physica* **17**, 272–281 (1951).

⁴R. J. S. Brown, *Nature* **189**, 387–388 (1961).

⁵E. Ragozzino, "Proton spin-lattice relaxation in solutions of glycerol in water," *Molecular Physics* **10**, 497–498 (1966).

⁶S.-W. Lo, G. J. Hirasaki, W. V. House, R. Kobayashi, *et al.*, "Correlations of nmr relaxation time with viscosity, diffusivity, and gas/oil ratio of methane/hydrocarbon mixtures," in *SPE Annual Technical Conference and Exhibition* (Society of Petroleum Engineers, 2000).

Appendix A: Schematic of Experimental Apparatus

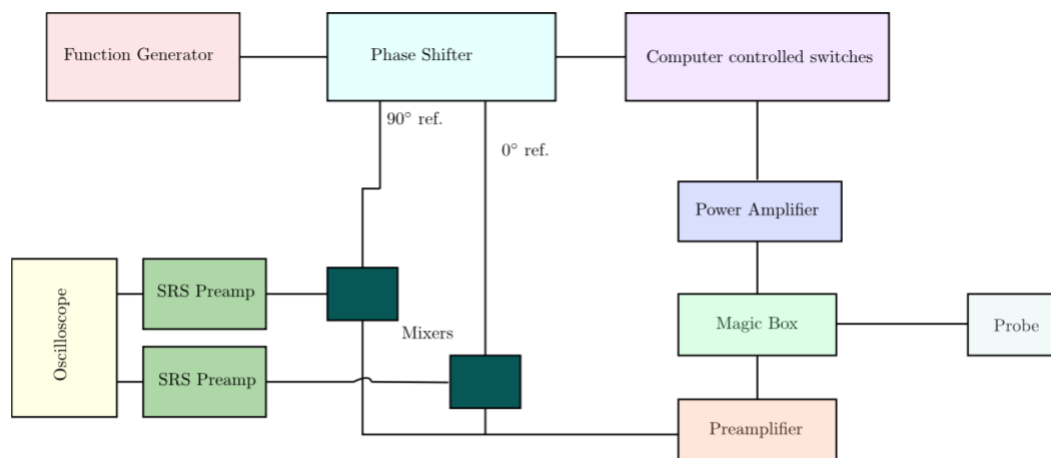


FIG. 5. Schematic block diagram of our experimental apparatus. The electromagnets generating B_z are not shown. In logical order: the function generator outputs a 6.436356 MHz sine wave with an amplitude of 3.25V peak-to-peak; the phase shifter splits this into two signals, 90° offset from one another for reference; the non-phase-shifted signal is shaped into pulses by the computer controlled switches; this pulse is amplified and delivered to the sample through the "Magic box" and the probe; the sample's response is captured by the probe and sent through the preamplifier; the amplified signal is then mixed with the reference signals from the phase shifter, amplified once again, and displayed on the oscilloscope for measurement.